

EXCLUSIVE HADRON BRANCHING RATIOS OF THE D MESON

LEBC-EHS Collaboration

M. Aguilar-Benitez¹⁰, W.W.M. Allison¹², J.L. Bailly¹¹, S. Banerjee³, W. Bartl²³,
M. Begalli¹, P. Beillière⁶, R. Bizzarri¹⁵, H. Briand¹⁴, R. Brun⁵, V. Canale¹⁵,
C. Caso⁸, E. Castelli²², P. Checchia¹³, P.V. Chliapnikov¹⁸, N. Colino¹⁰,
S.J. Colwill¹², R. Contri⁸, D. Crennell¹⁶, A. De Angelis¹³, L. de Billy¹⁴,
C. Defoix⁶, R. Di Marco¹⁷, E. Di Capua¹⁵, F. Diez-Hedo¹⁰, J. Dolbeau⁶,
J. Duboc¹⁴, J. Dumarchez¹⁴, M. Eriksson¹⁹, S. Falciano¹⁵, C. Fernandez⁵,
C. Fisher¹⁶, Yu.V. Fisyak¹⁸, F. Fontanelli⁸, J. Fry⁹, S.N. Ganguli³, U. Gasparini¹³,
U. Gensch², S. Gentile¹⁵, D.B. Gibaut¹², A.T. Goshaw⁷, R. Hamatsu²¹, L. Haupt¹⁹,
S. Hellman¹⁹, V. Henri¹¹, J.J. Hernandez⁵, S.O. Holmgren¹⁹, M. Houlden⁹,
J. Hrubec²³, P. Hughes¹⁶, D. Huss²⁰, Y. Iga²¹, M. Iori⁵, E. Jegham²⁰,
K.E. Johansson¹⁹, M.I. Josa¹⁰, M. Kalelkar¹⁷, A.G. Kholodenko¹⁸,
E.P. Kistenev¹⁸, S. Kitamura²¹, D. Knauss², V.V. Kniazev¹⁸, W. Kowald⁷,
D. Kuhn²³, J. Laberrigue¹⁴, M. Laloum⁶, P. Legros¹¹, H. Leutz⁵, L. Lyons¹²,
M. MacDermott¹⁶, P.K. Malhotra³, P. Mason⁹, M. Mazzucato¹³,
M.E. Michalon-Mentzer²⁰, A. Michalon²⁰, T. Moa¹⁹, R. Monge⁸, L. Montanet⁵,
G. Neuhofer²³, H.K. Nguyen¹⁴, S. Nilsson¹⁹, H. Nowak², N. Oshima²¹, G. Otter¹,
R. Ouared¹⁴, J. Panella Comellas¹², G. Patel⁹, C. Patrignani¹⁵, M. Pernicka²³,
P. Pilette¹¹, C. Pinori¹³, G. Piredda¹⁵, R. Plano¹⁷, A. Poppleton⁵,
P. Poropat²², S. Reucroft⁵, K. Roberts⁹, W.J. Robertson⁷, H. Rohringer²³,
J.M. Salicio¹⁰, R. Schulte¹, B. Sellden¹⁹, M. Sessa²², S. Squarcia⁸, P. Stamer¹⁷,
V.A. Stopchenko¹⁸, K. Takahashi²¹, M.C. Touboul⁵, U. Trevisan⁸,
C. Troncon²², T. Tsurugai²¹, L. Ventura¹³, P. Vilain⁴, E.V. Vlasov¹⁸,
C. Voltolini²⁰, B. Vonck⁴, W.D. Walker⁷, C.F. Wild⁷, T.P. Yiou¹⁴ and G. Zumerle¹³

Submitted to Zeitschrift für Physik C

- 1 III. Physikalisches Inst. der Technischen Hochschule, Aachen, Germany
- 2 Institute für Hochenergiephysik der AdW der DDR, Berlin-Zeuthen, GDR
- 3 Tata Institute of Fundamental Research, Bombay, India
- 4 IIHE ULB-VUB, Brussels, Belgium
- 5 CERN, European Organization for Nuclear Research, Geneva, Switzerland
- 6 Lab. de Physique Corpusculaire, Collège de France, Paris, France
- 7 Duke University, Durham, NC, USA
- 8 Dipartimento di Fisica and INFN, Università di Genova, Genova, Italy
- 9 Phys. Dept. University of Liverpool, Liverpool, UK
- 10 CIEMAT-JEN, Madrid, Spain
- 11 Université de l'Etat à Mons, Mons, Belgium
- 12 Nuclear Physics Laboratory, University of Oxford, Oxford, UK
- 13 Dipartimento di Fisica, Università di Padova and INFN, Padova, Italy
- 14 LPNHE, Paris 6-Paris 7, Paris, France
- 15 Dipartimento di Fisica and INFN, Università of Roma, La Sapienza, Roma, Italy
- 16 Rutherford and Appleton Laboratory, Chilton, UK
- 17 Rutgers University, New Brunswick, USA
- 18 Institute for High Energy Physics, Serpukhov, USSR
- 19 Institute of Physics, University of Stockholm, Sweden
- 20 Div. High Energy, CRN Strasbourg and Université Louis Pasteur, Strasbourg, France
- 21 Tokyo University of Agriculture and Technology and Tokyo Metropolitan University, Tokyo, Japan
- 22 Dipartimento di Fisica and INFN, Università Trieste, Trieste, Italy
- 23 Inst. für Hochenergiephysik der Osterreichischen Akademie der Wissenschaften, Vienna, Austria

ABSTRACT

The measurement of 12 D^0 and 10 D^{\pm} exclusive branching ratios are presented. The analysis is based on 608 spatially resolved charm particle decays produced in 360 GeV/c π^-p and 400 GeV/c pp interactions.

1. Introduction

In this paper we report on the measurement of exclusive hadronic branching ratios of the charm D mesons produced in $\pi^- p$ interactions at 360 GeV/c and proton proton interactions at 400 GeV/c. The data have been collected in the experiment NA27 at the CERN SPS using the European Hybrid Spectrometer (EHS) [1]. The experimental set-up has been described in detail elsewhere [2]. We report briefly the main characteristics of the apparatus which are used in the following analysis:

- the high resolution rapid cycling bubble chamber (LEBC [2]) provides the proton target and the vertex detector with bubble diameter 17 μm and bubble density of 80/cm;
- a large angle multiparticle spectrometer situated downstream of the bubble chamber provides momentum measurement for charged particles with an accuracy of 0.8% over the momentum range 0.5 to 150 GeV/c;
- the pictorial large volume drift chamber ISIS[3] provides the charged particle identification by ionization sampling. The combination of ionization and momentum measurements is used to derive a probability for any given mass assignment;
- the detection of electrons and photons is provided by two lead glass electromagnetic calorimeters (IGD and FGD [1],[4]).

265,000 $\pi^- p$ interactions and 1,015,000 pp interactions in the fiducial volume were observed. The selection procedure described in [5] yields a charm sample of 114 events containing 183 charm decays from $\pi^- p$ interactions, and of 324 events with 425 charm decays from pp interactions. We label Cn and Vn respectively the decays of charged and neutral particles into n charged decay products.

2. Sample reduction

We restrict the analysis to the events in the charm sample fulfilling the following requirements:

- the decay vertex is not obscured within $7\mu m$ [6] by a track from primary interaction;
- all charged decay products are reconstructed in the spectrometer;
- in the *V2* sample, one decay charged particle has transverse momentum greater than $250 MeV/c$;
- the decay is inside a cylinder of radius R centered around the incident beam particle ("charm box" see [2]);
- the decay length is less than L and greater than l , where L and l are defined in Tab. 1;
- similarly the minimum impact parameter (see Fig. 1 for definition) is greater than t , and the maximum is less than T and greater than T .

These cuts guarantee high detection efficiency and clear topology definition. They essentially remove the contamination from nuclear interactions, strange particle decays, and short-lived charm particles such as Λ_c or D_s . The following analysis is limited to the *V2* and *V4* samples for D^0 and to the *C3* sample for D^\pm . The *C1* sample is ignored since the systematic detection uncertainty is not well understood. The *C5* and *V6* topologies are ignored (poor statistics information).

The strange particle background in our *V2* sample, due to a wrong association of a track between the bubble chamber and the spectrometer [2] giving an apparent transverse momentum greater than $250 MeV/c$ is of the order of 2%. For *C3* and *V4* this contamination is completely negligible. For the *C3* sample we analyzed by Monte-Carlo the effects of our cuts in eliminating Λ_c . Using the production properties [5] and the lifetime of Λ_c measured by our experiment [7], we estimate at most that the Λ_c contamination in the *C3* sample is 5%.

This selection yields a sample of 106 *V2*, 68 *C3* and 34 *V4* decays (see Tab. 2).

3. Mean decay multiplicities.

We first consider decay multiplicities for charged and neutral D mesons. Fig. 2.a,b,c show the distributions of $P_{t_{max}}$, the maximum transverse momentum of the charged decay products with respect to the parent particle for V2,C3 and V4, respectively (decays with good 3C fits, i.e. no missing neutrals, were excluded). It turns out that the shape of these distributions depends on the number of unseen neutral products but not on the identity of these decay products. A maximum likelihood fit[7] to the data, using phase space Monte-Carlo distributions and taking into account the 3C fit decays, gives the following mean decay multiplicities:

$$3.4 \pm 0.2 \text{ in V2}$$

$$4.1 \pm 0.2 \text{ in C3}$$

$$4.6^{+0.2}_{-0.1} \text{ in V4}$$

The errors include uncertainties due to final state interaction, like ρ and K^* resonances, as well as the presence of semileptonic decays.

4. Exclusive branching ratios

We first consider exclusive branching ratios to all charged final states for D^0 and D^\pm . We require a unique three constraint (3C) kinematic fit. In Tab. 3 we give the number of these fits obtained for each decay mode. They yield:*

$$\frac{B.R.(D^0 \rightarrow K^- \pi^+)}{B.R.(D^0 \rightarrow 2 \text{ charged})} = 5.8^{+3.0\%}_{-1.4\%}$$

$$\frac{B.R.(D^0 \rightarrow \pi^- \pi^+)}{B.R.(D^0 \rightarrow 2 \text{ charged})} = 0.8^{+1.8\%}_{-0.3\%}$$

$$\frac{B.R.(D^0 \rightarrow K^- \pi^- \pi^+ \pi^+)}{B.R.(D^0 \rightarrow 4 \text{ charged})} = 38.2^{+10.0\%}_{-6.5\%}$$

$$\frac{B.R.(D^0 \rightarrow \pi^- \pi^- \pi^+ \pi^+)}{B.R.(D^0 \rightarrow 4 \text{ charged})} = 2.9^{+6.4\%}_{-0.9\%}$$

* In all the analysis the statistical errors correspond to a symmetric confidence interval of 68% evaluated using the binomial distribution.

$$\frac{B.R.(D^+ \rightarrow K^- \pi^+ \pi^+)}{B.R.(D^+ \rightarrow 3 \text{ charged})} = 11.8^{+5.3\%}_{-2.7\%}$$

$$\frac{B.R.(D^+ \rightarrow K^- K^+ \pi^+)}{B.R.(D^+ \rightarrow 3 \text{ charged})} = 1.5^{+3.3\%}_{-0.4\%}$$

where the corrections due to the selection criteria are taken into account. The errors include statistical and systematic uncertainties. Combining these results with the topological branching ratios given in [7]:

$$B.R.(D^0 \rightarrow 2 \text{ charged}) = 0.69 \pm 0.04$$

$$B.R.(D^0 \rightarrow 4 \text{ charged}) = 0.17 \pm 0.03$$

$$B.R.(D^+ \rightarrow 3 \text{ charged}) = 0.52 \pm 0.09$$

we finally obtain the exclusive absolute branching ratios listed in Tab. 3.

To evaluate the branching ratios for decay modes involving neutral products we use a different approach not related to kinematic fits, since the neutral particles are detected with low efficiency in this experiment. The following invariant quantity is evaluated:

$$m_{om}^2 = m_i^2 + m_c^2 - 2m_i \sqrt{m_c^2 + p_i^2}$$

where m_i is the mass of the incident charm particle, m_c the effective mass of the charged final state and p_i the transverse momentum of this system. The value of m_{om}^2 strongly depends on the number of unseen neutral products, as can be seen in Fig. 3a. This allows to discriminate statistically between decays with one or more than one neutral product. From the cumulative distributions we can define a discriminating value $m_{om}^2 \text{ cut}$ and a probability (p). A decay is attributed one or more than one missing neutral particle, with probability p , when m_{om}^2 is lower or greater than $m_{om}^2 \text{ cut}$ [5],[9], respectively. The $m_{om}^2 \text{ cut}$ and p are evaluated by simulating decays for different topologies (see Tab. 4).

To evaluate m_{om}^2 we need to identify the charged decay products. A particle is defined as uniquely identified by ISIS if the probability of one mass hypothesis is greater than 5%, the others being less than 5% [2]. The systematic error introduced by this criterium is $\approx 5\%$. We restrict our analysis to decays in the $V2$ and $C3$ samples satisfying the following additional requirements:

- in the $V2$ sample, both charged particles must be uniquely identified;
- in the $C3$ sample, the particle with opposite charge to the parent particle must be uniquely identified.

We assume that the contribution of Cabibbo suppressed decay modes (expected to be of the order of 5%) is small compared to the statistical uncertainties, and can be neglected.

We observed 7 semielectronic decays (e.g. with a track uniquely identified as electron by ISIS), 4 V2 and 3 C3. Monte-Carlo simulations show that the semielectronic decays can be treated as the hadronic ones in the $m_{o,m}^2$ analysis, thus we include them in the sample. Tab. 5 gives the characteristics of the selected samples, and Fig. 4.a,b,c,d the experimental $m_{o,m}^2$ distributions for V2 $K^-\pi^+$, V2 $\pi^+\pi^-$, C3 $K^-\pi^+\pi^+$, and C3 $\pi^-\pi^+\pi^+$ respectively.

Particle identification in NA27 has a poor discriminating power for muons versus pions. There are no reported data at present [8] on D meson exclusive B.R. in semimuonic final states. Assuming electron-muon universality, the number of semileptonic decays in muons must be equal to the number of observed semielectronic decays with identical decay multiplicities. One can therefore correct for muon contamination in hadronic decay modes. Once all the corrections are taken into account, one finds:

$$\frac{B.R.(D^0 \rightarrow K^-\pi^+\pi^0)}{B.R.(D^0 \rightarrow 2 \text{ charged})} = 15.4^{+8.9\%}_{-4.0\%}$$

$$\frac{B.R.(D^0 \rightarrow K^-\pi^+ + 2 \div 3 \pi^0)}{B.R.(D^0 \rightarrow 2 \text{ charged})} = 30.3^{+10.7\%}_{-6.2\%}$$

$$\frac{B.R.(D^0 \rightarrow K^-e^+\nu)}{B.R.(D^0 \rightarrow 2 \text{ charged})} < 6.8\% \quad (90\% \text{ C.L.})$$

$$\frac{B.R.(D^0 \rightarrow K^-e^+\nu + 1, 2\pi^0)}{B.R.(D^0 \rightarrow 2 \text{ charged})} = 3.2^{+7.3\%}_{-0.9\%}$$

$$\frac{B.R.(D^0 \rightarrow \bar{K}^0\pi^-\pi^+)}{B.R.(D^0 \rightarrow 2 \text{ charged})} = 6.6^{+8.6}_{-2.0}$$

$$\frac{B.R.(D^0 \rightarrow \bar{K}^0\pi^-\pi^+ + 1 \div 2\pi^0)}{B.R.(D^0 \rightarrow 2 \text{ charged})} = 15.3^{+10.6\%}_{-4.0\%}$$

$$\frac{B.R.(D^0 \rightarrow \pi^-e^+\nu)}{B.R.(D^0 \rightarrow 2 \text{ charged})} < 7.3\% \quad (90\% \text{ C.L.})$$

$$\frac{B.R.(D^0 \rightarrow \bar{K}^0\pi^-e^+\nu)}{B.R.(D^0 \rightarrow 2 \text{ charged})} = 11.5^{+10.0\%}_{-3.3\%}$$

$$\frac{B.R.(D^+ \rightarrow K^-\pi^+\pi^-\pi^0)}{B.R.(D^+ \rightarrow 3 \text{ charged})} = 4.2^{+8.9\%}_{-1.2\%}$$

$$\frac{B.R.(D^+ \rightarrow K^-\pi^+\pi^+\pi^0\pi^0)}{B.R.(D^+ \rightarrow 3 \text{ charged})} = 4.2^{+8.9\%}_{-1.2\%}$$

$$\frac{B.R.(D^+ \rightarrow K^-e^+\pi^+\nu)}{B.R.(D^+ \rightarrow 3 \text{ charged})} < 9.2\% \quad (90\% \text{ C.L.})$$

$$\frac{B.R.(D^+ \rightarrow K^-e^+\pi^+\nu\pi^0)}{B.R.(D^+ \rightarrow 3 \text{ charged})} = 8.3^{+9.9\%}_{-2.5\%}$$

$$\frac{B.R.(D^+ \rightarrow \bar{K}^0 \pi^- \pi^+ \pi^+)}{B.R.(D^+ \rightarrow 3 \text{ charged})} = 45.8^{+12.1\%}_{-7.8\%}$$

$$\frac{B.R.(D^+ \rightarrow \bar{K}^0 \pi^- \pi^+ \pi^0)}{B.R.(D^+ \rightarrow 3 \text{ charged})} = 8.3^{+9.9\%}_{-2.5\%}$$

$$\frac{B.R.(D^+ \rightarrow \pi^- e^+ \pi^+ \nu)}{B.R.(D^+ \rightarrow 3 \text{ charged})} < 9.2\% \quad (90\% \text{ C.L.})$$

$$\frac{B.R.(D^+ \rightarrow \bar{K}^0 \pi^- e^+ \pi^+ \nu)}{B.R.(D^+ \rightarrow 3 \text{ charged})} = 4.2^{+8.9\%}_{-1.2\%}$$

Using the topological branching ratios [7] given above, one finds the branching ratios listed in Tab. 6. In this reduced sample there are some decays with no neutral products and the corresponding branching ratios are consistent with the result obtained previously using the information of the kinematic fits.

From the results of Tab. 5 we can also evaluate the decay multiplicities in the V2 and C3 samples. The results are in agreement with the values obtained in the maximum transverse momentum analysis.

We can also give an estimation of inclusive D mesons branching ratios in kaon and electron to be compared with the result of the statistical analysis [7](see Tab. 7). The two methods give consistent results.

In conclusion we have presented results on exclusive branching ratios for 12 decay modes of the D^0 , and 10 decay modes of the D^\pm . Our results cover the 68% of the D^0 decay modes and the 47% of the D^\pm and they are summarized in Tab. 8. For comparison, we reproduce in Tab. 9 the results obtained by MARK III on the same final states [11]. The two sets of data are in good agreement.

REFERENCES

- [1] M. Aguilar-Benitez et al., Nucl. Instr. Meth. 205 (1983) 79.
- [2] M. Aguilar-Benitez et al., to be published in Nucl. Instr. Meth.
- [3] W.W. Allison et al., Nucl. Instr. Meth. 224 (1984) 396.
- [4] B. Powell et al., Nucl. Instr. Meth. 198 (1982) 217.
- [5] M. Aguilar-Benitez et al., Z. Phys. C31 (1986) 491.
- [6] J.R. Lutz and A. Michalon: II Vezelay Workshop on EHS, CERN/EP-EHS/PH 80-2.
- [7] M. Aguilar-Benitez et al., Inclusive D meson branching ratios, to be submitted to Z. Phys. C.
- [8] Particle Data Group, Review of Particle Properties, Phys. Lett. 170B (1986).
- [9] M. Aguilar-Benitez et al., Z. Phys. C34 (1987) 143.
- [10] M. Aguilar-Benitez et al., Phys. Lett. 168B (1986) 170.
- [11] Presented at the Rencontre de Moriond, March 1987.

TABLE CAPTIONS

- Tab. 1 Topology dependent cuts applied to select the sample.
- Tab. 2 Sample reduction.
- Tab. 3 Branching ratios for 3C fit final states.
- Tab. 4 For a given mass assignment to the charged system a decay is supposed to have one or more than one neutral missing with probability p when its m_{om}^2 is lower or greater than m_{omcut}^2 .
- Tab. 5 Selection of events for m_{om}^2 analysis.
- Tab. 6 Number of events for decay modes involving neutrals and the corresponding branching ratios.
- Tab. 7 Comparison of inclusive B.R. obtained in the present analysis and the analogous result obtained using a different method [7].
- Tab. 8 Exclusive branching ratios in the experiment NA27.
- Tab. 9 Comparison of result with MARK III data [11].

Table 1

Top.	R (mm)	$L > \text{lenght} > l$ (cm)		$\tau > Y_{max} > T$ (μm)		$Y_{min} > t$ (μm)
V2	0.2	3.0	0.1	500	25	7
C3	2.0	—	0.1	2000	80	7
V4	2.0	—	0.1	1500	25	7

Table 2

Topology	Full sample	All charged hybridized	Inside cuts
V2	244	191	106
C3	185	103	68
V4	74	45	34

Table 3

Decay mode	n° of fits	B.R. %
$D^0 \rightarrow K^- \pi^+$	7	$4.0^{+2.1}_{-1.0} \pm 0.2$
$D^0 \rightarrow \pi^- \pi^+$	1	$0.5^{+1.2}_{-0.2} \pm 0.04$
$D^0 \rightarrow K^- \pi^- \pi^+ \pi^+$	13	$6.5^{+1.7}_{-1.1} \pm 1.9$
$D^0 \rightarrow \pi^- \pi^- \pi^+ \pi^+$	1	$0.5^{+1.1}_{-0.1} \pm 0.1$
$D^+ \rightarrow K^- \pi^+ \pi^+$	8	$6.3^{+2.8}_{-1.4} \pm 1.1$
$D^+ \rightarrow K^- K^+ \pi^+$	1	$0.8^{+1.7}_{-0.2} \pm 0.1$

Table 4

Charged system	m_{oMcut}^2 (GeV ² /c ²)	P %
$K^- \pi^+$	0.25	80
$\pi^- \pi^+$	0.65	80
$K^- \pi^+ \pi^+$	0.15	85
$\pi^- \pi^+ \pi^+$	0.55	85

Table 5

Events selected	3C fits	Requiring neutrals	Charged mass	Single neutral	Multi-neutral
30	1 $K^- \pi^+$ 1 $\pi^- \pi^+$	28	$K^- \pi^+$	6	9
			$K^- e^+$	0	1
			$\pi^- \pi^+$	3	6
			$\pi^- e^+$	0	3
24	3 $K^- \pi^+ \pi^+$	21	$K^- \pi^+ \pi^+$	1	3
			$K^- \pi^+ e^+$	0	2
			$\pi^- \pi^+ \pi^+$	10	4
			$\pi^- \pi^+ e^+$	0	1

Table 6

Decay mode	n° of corrected events	B.R. %
$D^0 \rightarrow K^- \pi^+ \pi^0$	5	$10.6^{+6.1}_{-2.8} \pm 0.6$
$D^0 \rightarrow K^- \pi^+ + 2, 3 \pi^0$	9	$20.9^{+7.4}_{-4.3} \pm 1.2$
$D^0 \rightarrow K^- e^+ \nu$	0	< 5.0 *
$D^0 \rightarrow K^- e^+ \nu + 1, 2 \pi^0$	1	$2.3^{+5.0}_{-0.6} \pm 0.1$
$D^0 \rightarrow \bar{K}^0 \pi^- \pi^+$	2	$4.5^{+5.9}_{-1.4} \pm 0.3$
$D^0 \rightarrow \bar{K}^0 \pi^- \pi^+ + 1, 2 \pi^0$	4	$10.6^{+7.8}_{-2.9} \pm 0.6$
$D^0 \rightarrow \pi^- e^+ \nu$	0	< 5.4 *
$D^0 \rightarrow \bar{K}^0 \pi^- e^+ \nu + 0, 1 \pi^0$	3	$7.9^{+6.9}_{-2.8} \pm 0.5$
$D^+ \rightarrow K^- \pi^+ \pi^+ \pi^0$	1	$2.2^{+4.7}_{-0.6} \pm 0.4$
$D^+ \rightarrow K^- \pi^+ \pi^+ \pi^0 \pi^0$	1	$2.2^{+4.7}_{-0.6} \pm 0.4$
$D^+ \rightarrow K^- \pi^+ e^+ \nu$	0	< 5.7 *
$D^+ \rightarrow K^- \pi^+ e^+ \nu \pi^0$	2	$4.4^{+5.2}_{-1.3} \pm 0.7$
$D^+ \rightarrow \bar{K}^0 \pi^- \pi^+ \pi^+$	11	$24.3^{+6.4}_{-4.1} \pm 4.1$
$D^+ \rightarrow \bar{K}^0 \pi^- \pi^+ \pi^+ \pi^0$	2	$4.4^{+5.2}_{-1.3} \pm 0.7$
$D^+ \rightarrow \pi^- \pi^+ e^+ \nu$	0	< 5.7 *
$D^+ \rightarrow \bar{K}^0 \pi^- \pi^+ e^+ \nu$	1	$2.2^{+4.7}_{-0.6} \pm 0.4$

* 90% C.L. upper limit

Table 7

Topology	Inclusive B.R.	present analysis	ref [7]
V2	$\frac{B.R.(D^0 \rightarrow e^\pm + X)}{B.R.(D^0 \rightarrow 2 \text{ charged})}$	$0.15^{+0.10}_{-0.04}$	$0.21^{+0.08}_{-0.06}$
	$\frac{B.R.(D^0 \rightarrow K^\pm + X)}{B.R.(D^0 \rightarrow 2 \text{ charged})}$	$0.53^{+0.10}_{-0.07}$	$0.46^{+0.10}_{-0.09}$
C3	$\frac{B.R.(D^\pm \rightarrow e^\pm + X)}{B.R.(D^\pm \rightarrow 3 \text{ charged})}$	$0.13^{+0.11}_{-0.04}$	$0.12^{+0.08}_{-0.06}$
	$\frac{B.R.(D^\pm \rightarrow K^\mp + X)}{B.R.(D^\pm \rightarrow 3 \text{ charged})}$	$0.38^{+0.12}_{-0.07}$	$0.33^{+0.12}_{-0.11}$

Table 8

$D^0 \rightarrow$	B.R. (%)	$D^+ \rightarrow$	B.R. (%)
$K^- \pi^+$	$4.0^{+2.1}_{-1.0} \pm 0.2$	$K^- \pi^+ \pi^+$	$6.3^{+2.8}_{-1.4} \pm 1.1$
$\pi^- \pi^+$	$0.5^{+1.2}_{-0.2} \pm 0.04$	$K^- K^+ \pi^+$	$0.8^{+1.7}_{-0.2} \pm 0.1$
$K^- \pi^+ \pi^0$	$10.6^{+6.1}_{-2.8} \pm 0.6$	$K^- \pi^+ \pi^- \pi^0$	$2.2^{+4.7}_{-0.6} \pm 0.4$
$\bar{K}^0 \pi^+ \pi^-$	$4.5^{+5.9}_{-1.4} \pm 0.3$	$\bar{K}^0 \pi^- \pi^+ \pi^+$	$24.3^{+6.4}_{-4.1} \pm 4.1$
$K^- \pi^+ + 2,3 \pi^0$	$20.9^{+7.4}_{-4.3} \pm 1.2$	$K^- \pi^+ \pi^+ \pi^0 \pi^0$	$2.2^{+4.7}_{-0.6} \pm 0.4$
$\bar{K}^0 \pi^- \pi^+ + 1,2 \pi^0$	$10.6^{+7.3}_{-2.9} \pm 0.6$	$\bar{K}^0 \pi^- \pi^+ \pi^+ \pi^0$	$4.4^{+5.2}_{-1.3} \pm 0.7$
$K^- \pi^- \pi^+ \pi^+$	$6.5^{+1.7}_{-1.1} \pm 1.9$	$K^- \pi^+ e^+ \nu_e$	$< 5.7^*$
$\pi^- \pi^- \pi^+ \pi^+$	$0.5^{+1.1}_{-0.1} \pm 0.1$	$K^- \pi^+ e^+ \nu_e \pi^0$	$4.4^{+5.2}_{-1.3} \pm 0.7$
$K^- e^+ \nu_e$	$< 5.0^*$	$\pi^- \pi^+ e^+ \nu_e$	$< 5.7^*$
$K^- e^+ \nu_e + 1,2 \pi^0$	$2.3^{+5.0}_{-0.6} \pm 0.1$	$\bar{K}^0 \pi^- \pi^+ e^+ \nu_e$	$2.2^{+4.7}_{-0.6} \pm 0.4$
$\pi^- e^+ \nu_e$	$< 5.4^*$		
$\bar{K}^0 \pi^- e^+ \nu_e + 0,1 \pi^0$	$7.9^{+6.9}_{-2.3} \pm 0.5$		

* 90% C.L. upper limit

Table 9

Decay mode	NA27	MARK III
$K^-\pi^+$	$4.0^{+2.1}_{-1.0} \pm 0.2$	4.2 ± 0.4
$\pi^-\pi^+$	$0.5^{+1.2}_{-0.2} \pm 0.04$	0.18 ± 0.05
$K^-\pi^+\pi^0$	$10.6^{+6.1}_{-2.8} \pm 0.6$	13.3 ± 1.2
$\bar{K}^0\pi^+\pi^-$	$4.5^{+5.9}_{-1.4} \pm 0.3$	6.7 ± 1.9
$K^-\pi^+\pi^+\pi^-$	$6.5^{+1.7}_{-1.1} \pm 1.9$	9.1 ± 0.8
$\pi^-\pi^-\pi^+\pi^-$	$0.5^{+1.1}_{-0.1} \pm 0.1$	1.5 ± 0.6
$K^-\pi^+\pi^+$	$6.3^{+2.8}_{-1.4} \pm 1.1$	9.3 ± 1.4
$K^-K^+\pi^+$	$0.8^{+1.7}_{-0.2} \pm 0.1$	$< 1.6^*$
$K^-\pi^+\pi^-\pi^0$	$2.2^{+4.7}_{-0.6} \pm 0.4$	6.4 ± 1.5
$\bar{K}^0\pi^-\pi^+\pi^+$	$24.3^{+6.4}_{-4.1} \pm 4.1$	15.2 ± 5.8

* 90% C.L. upper limit

Figure captions

Fig. 1 Definition of impact parameter of a track with respect to the primary vertex

Fig. 2 Experimental $p_{t \text{ max}}$ distribution. The solid lines show the theoretical distributions depending on the number of neutrals.

2.a V2 sample

2.b C3 sample

2.c V4 sample

Fig. 3.a Theoretical $m_{o\pi}^2$ distribution for Cabibbo favoured decay modes (V2 sample)

Fig. 3.b Theoretical $m_{o\pi}^2$ cumulative distribution for Cabibbo favoured decay modes (V2 sample)

Fig. 4 Experimental $m_{o\eta}^2$ distribution:

a V2 sample $K^- \pi^+$

b V2 sample $\pi^- \pi^+$

c C3 sample $K^- \pi^+ \pi^+$

d C3 sample $\pi^- \pi^+ \pi^+$

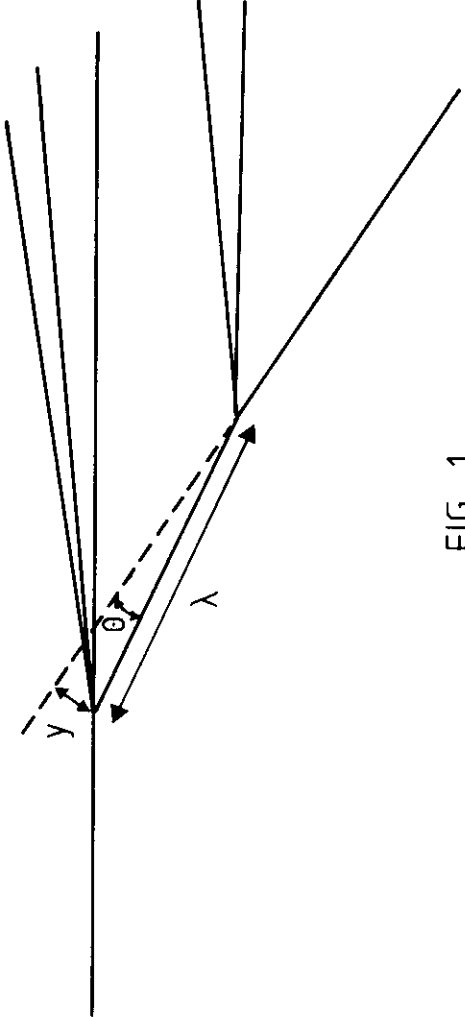


FIG. 1

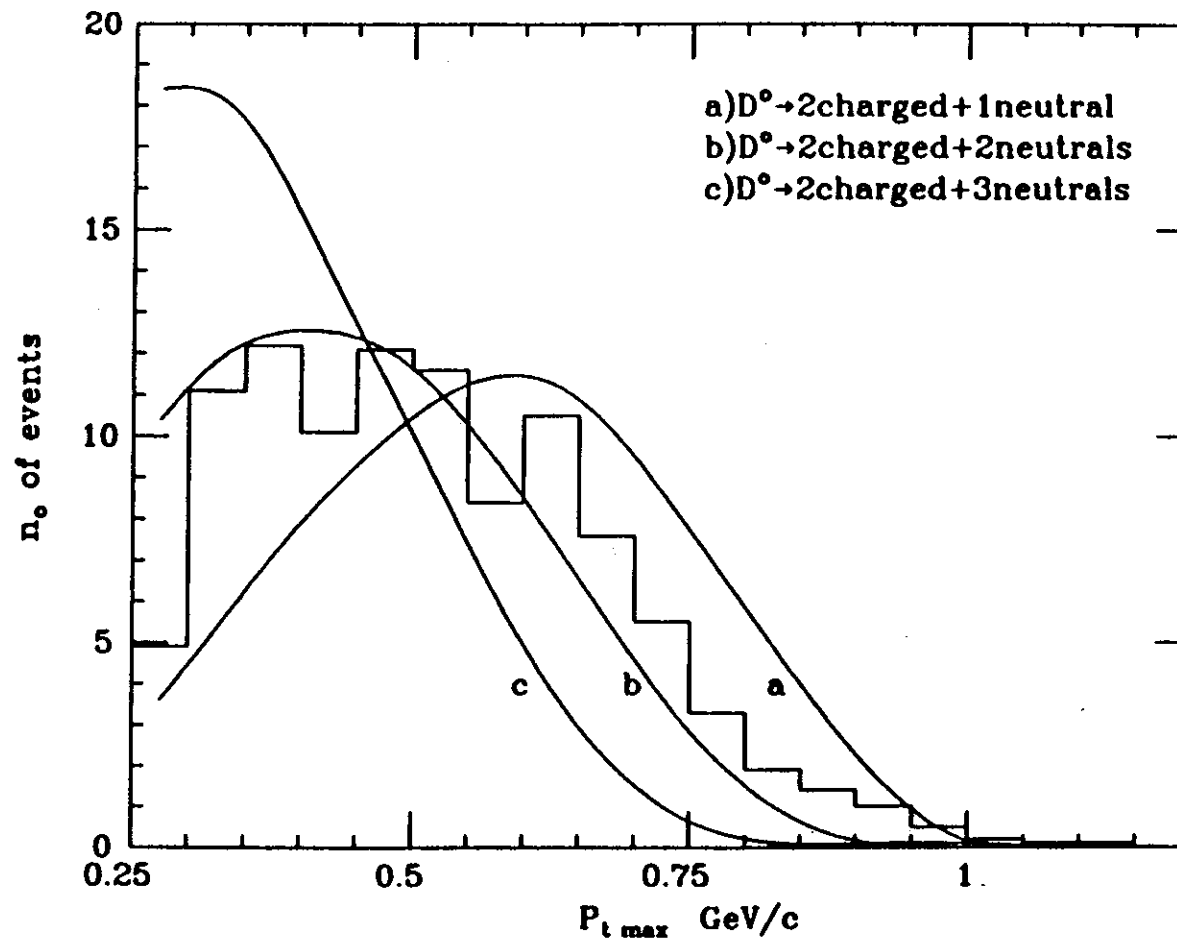


FIG. 2a

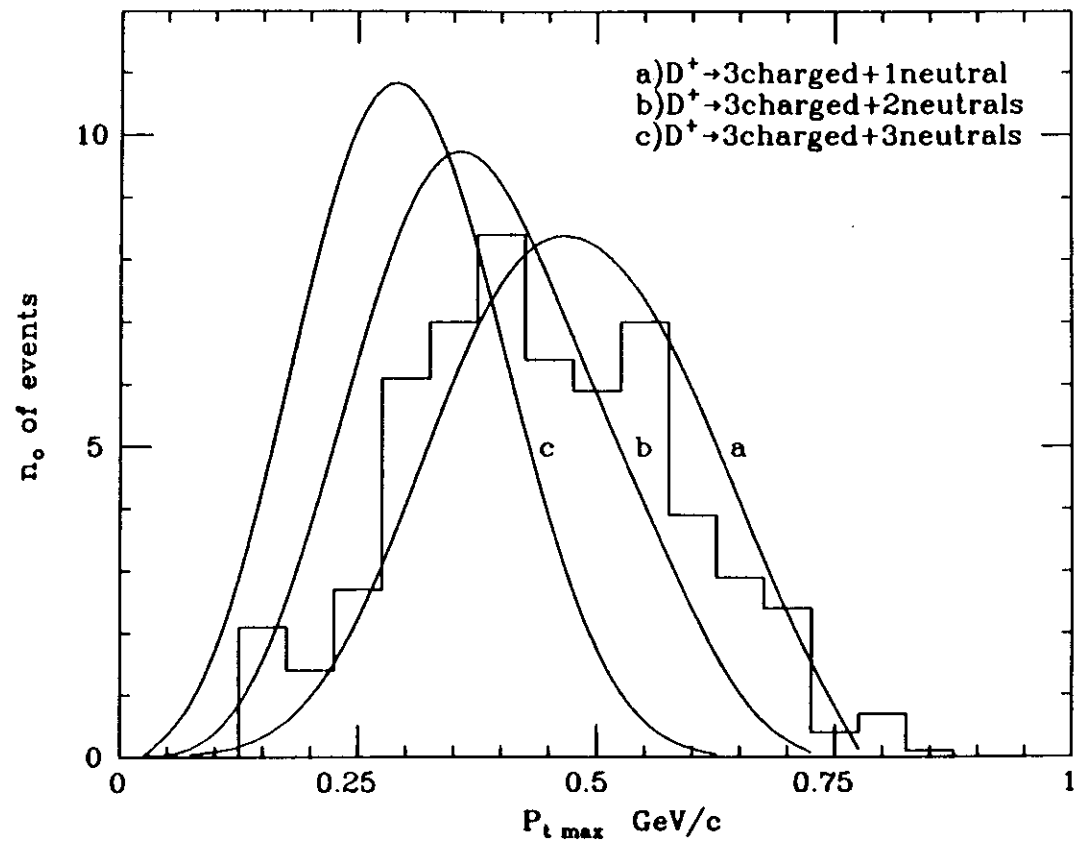


FIG. 2b

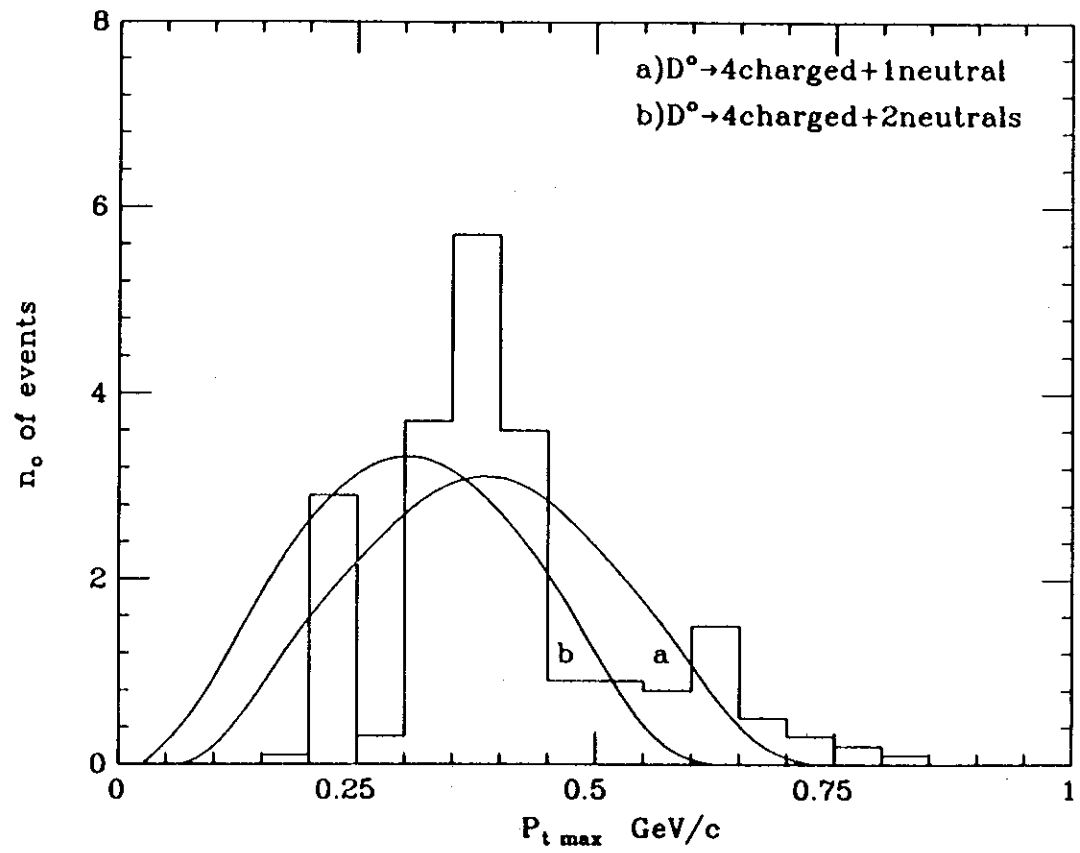


FIG. 2c

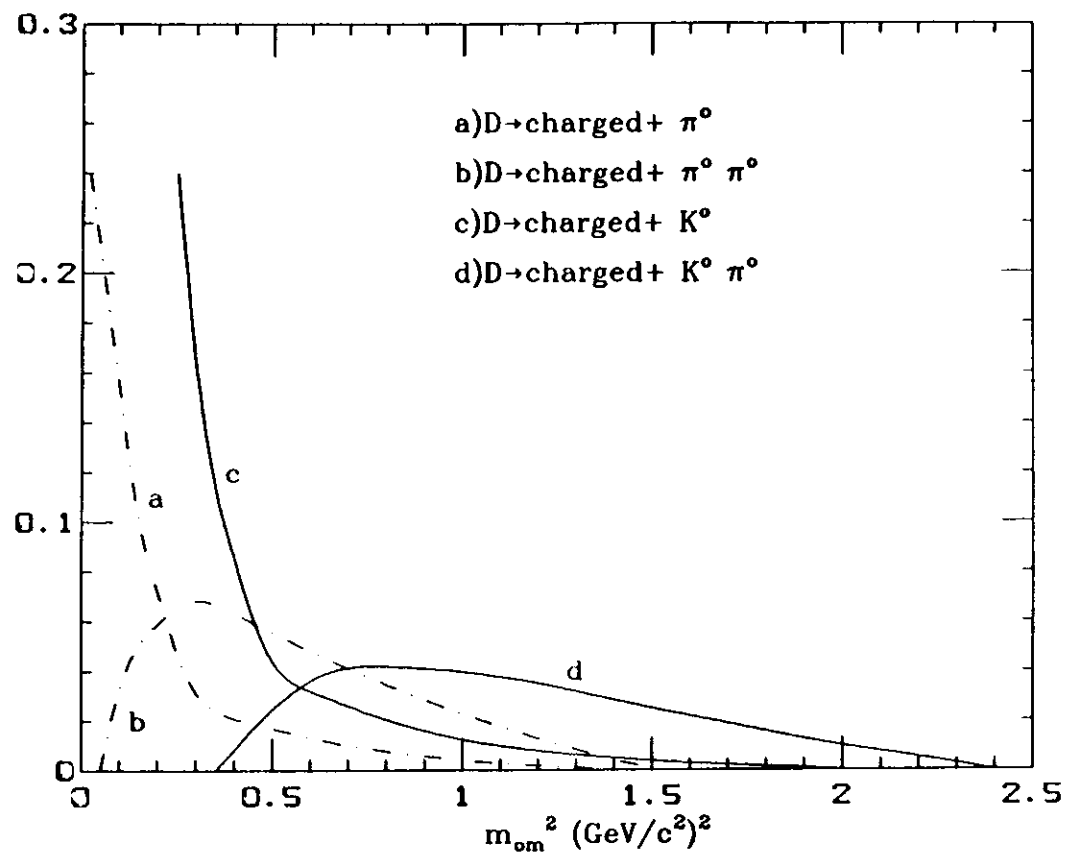


FIG. 3a

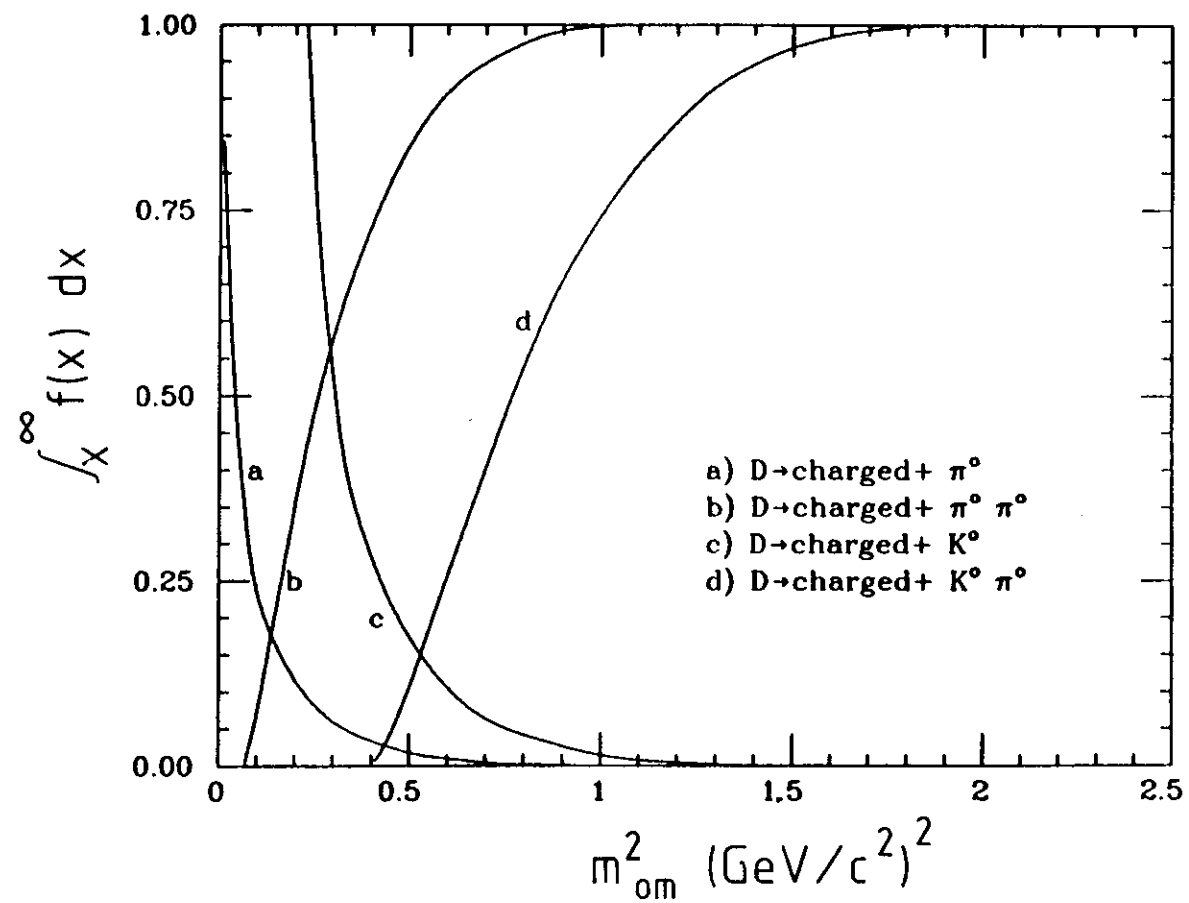


FIG. 3b

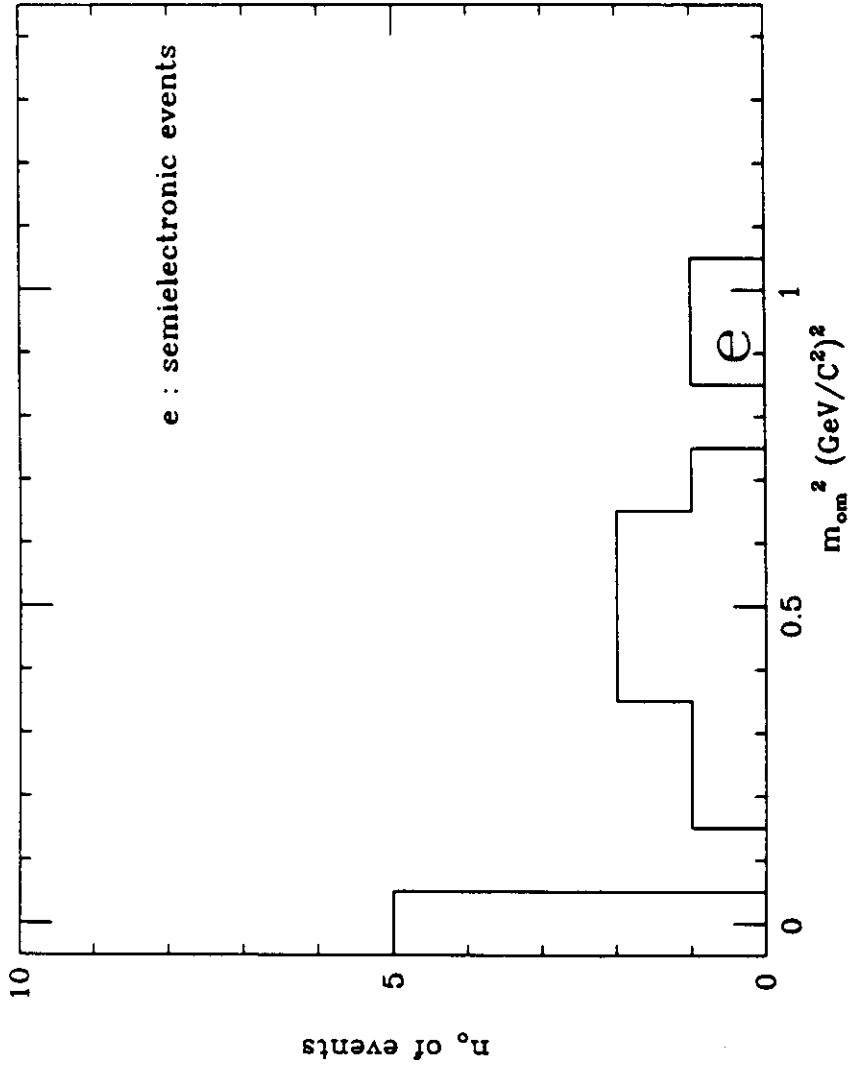


FIG. 4a

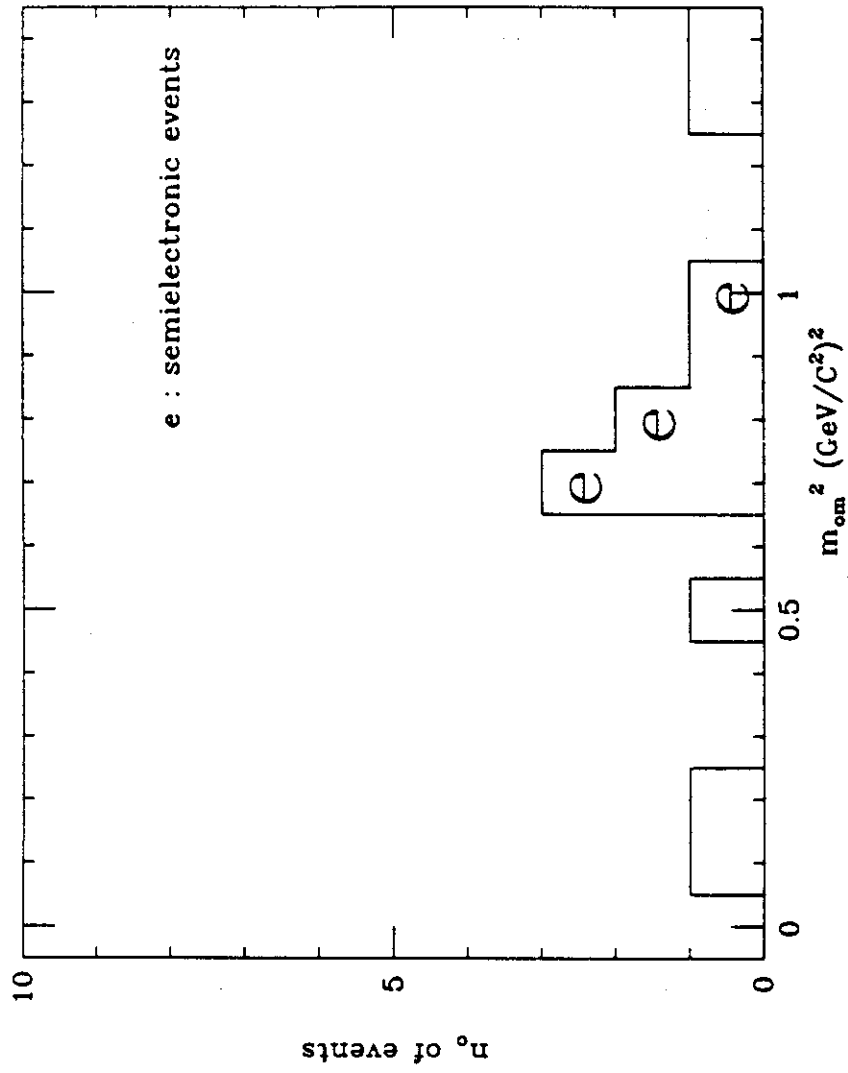


FIG. 4b

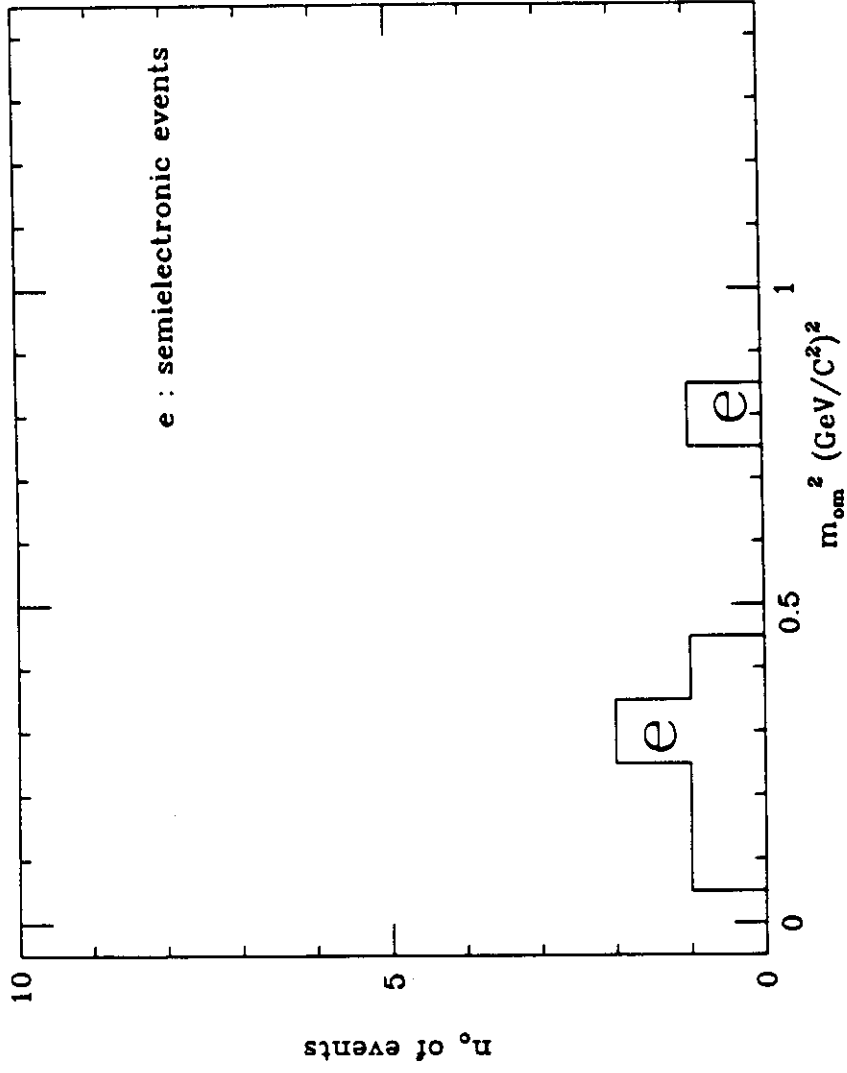


FIG. 4c

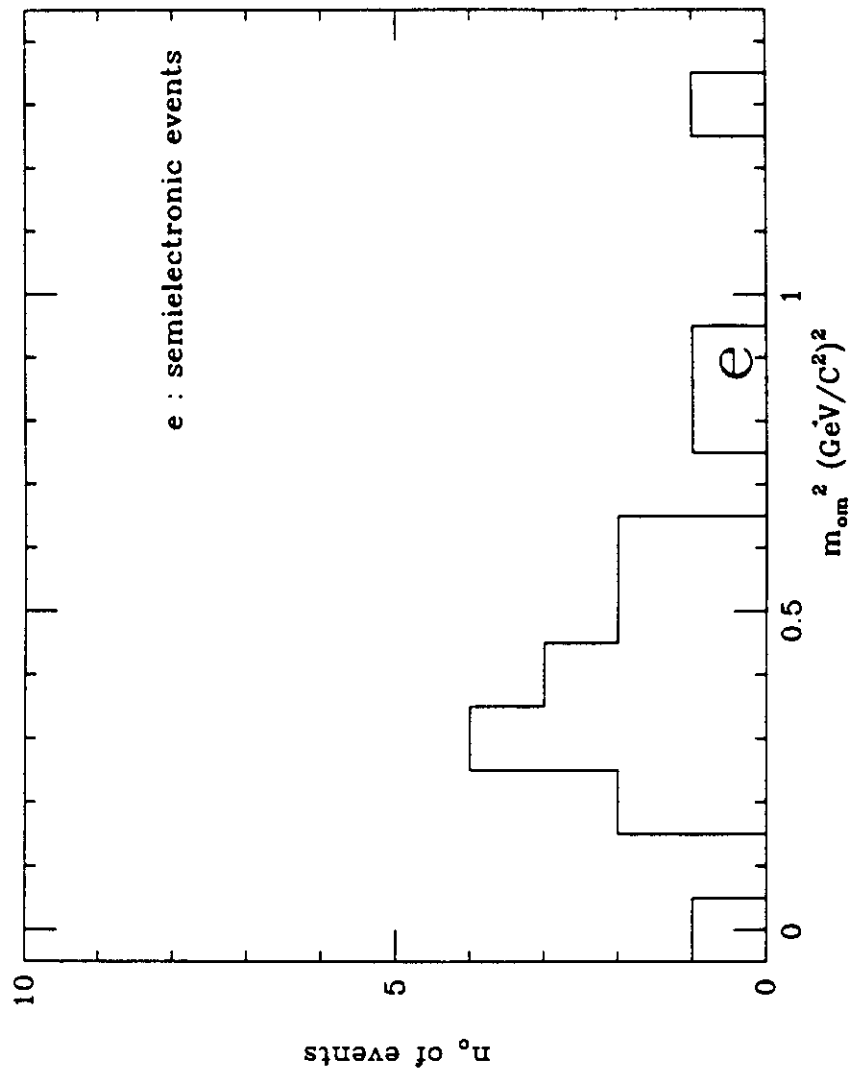


FIG. 4d